Hypocretin (orexin) is critical in sustaining theta/gamma-rich waking behaviors that drive sleep need

Anne Vassalli[a,b,1] and Paul Franken[a]

[a]Center for Integrative Genomics, University of Lausanne, CH-1015 Lausanne, Switzerland; and [b]Department of Physiology, University of Lausanne, CH-1005 Lausanne, Switzerland

Edited by Joseph S. Takahashi, Howard Hughes Medical Institute, University of Texas Southwestern Medical Center, Dallas, TX, and approved May 25, 2017 (received for review January 29, 2017)

Hcrt **gene inactivation in mice leads to behavioral state instability, abnormal transitions to paradoxical sleep, and cataplexy, hallmarks of narcolepsy. Sleep homeostasis is, however, considered unimpaired in patients and narcoleptic mice. We find that whereas** ***Hcrt*** $^{ko/ko}$ **mice respond to 6-h sleep deprivation (SD) with a slow-wave sleep (SWS) EEG δ (1.0 to 4.0 Hz) power rebound like** ***WT*** **littermates, spontaneous waking fails to induce a δ power reflecting prior waking duration. This correlates with impaired θ (6.0 to 9.5 Hz) and fast-γ (55 to 80 Hz) activity in prior waking. We algorithmically identify a theta-dominated wakefulness (TDW) substate underlying motivated behaviors and typically preceding cataplexy in** ***Hcrt*** $^{ko/ko}$ **mice.** ***Hcrt*** $^{ko/ko}$ **mice fully implement TDW when waking is enforced, but spontaneous TDW episode duration is greatly reduced. A reformulation of the classic sleep homeostasis model, where homeostatic pressure rises exclusively in TDW rather than all waking, predicts δ power dynamics both in** ***Hcrt*** $^{ko/ko}$ **and** ***WT*** **mouse baseline and recovery SWS. The low homeostatic impact of** ***Hcrt*** $^{ko/ko}$ **mouse spontaneous waking correlates with decreased cortical expression of neuronal activity-related genes (notably** ***Bdnf***, ***Egr1/Zif268***, **and** ***Per2***). **Thus, spontaneous TDW stability relies on Hcrt to sustain θ/fast-γ network activity and associated plasticity, whereas other arousal circuits sustain TDW during SD. We propose that TDW identifies a discrete global brain activity mode that is regulated by context-dependent neuromodulators and acts as a major driver of sleep homeostasis. Hcrt loss in** ***Hcrt*** $^{ko/ko}$ **mice causes impaired TDW maintenance in baseline wake and blunted δ power in SWS, reproducing, respectively, narcolepsy excessive daytime sleepiness and poor sleep quality.**

hypocretin/orexin | narcolepsy | sleep homeostasis | brain theta oscillations | waking substate

Wakefulness encompasses a wide spectrum of arousal levels, sensorimotor processing modes, and behaviors, reflected in the electroencephalogram (EEG) by a great variety of signal patterns (1). Fourier transform decomposes the signal into multiple frequency ranges, defining δ, θ (5 to 10 Hz), and γ (>30 Hz) oscillatory components. However, although the EEG has been used to define wakefulness and distinguish it from slow-wave and paradoxical sleep (SWS and PS) for decades, a formal cartography of waking substates, associated EEG features, and their significance for the animal is largely lacking. Likewise, definition of the relation between waking quality and subsequent sleep content has evolved little since enunciation of the two-process model of sleep regulation (2) in which a sleep/wake-dependent homeostatic "process *S*," reflected in EEG δ power during SWS, regulates sleep propensity as a function of prior waking duration regardless of waking quality. Later studies described behaviors (3, 4) or EEG components (5, 6) that disproportionally affect the sleep homeostat. Different procedural, cognitive, or emotional experience differentially impacts subsequent SWS δ power not only quantitatively but also spatially across brain areas, hence heralding sleep as a local, use-dependent process (7). If wake partly instructs sleep, is a formal modeling of the link between waking spectral dynamics and sleep spectral dynamics possible? Such insight may greatly further our understanding of sleep-need physiology.

Waking relies on wake-active cell populations in a set of key arousal centers (8). Among them, Hcrt cells in lateral hypothalamus (9), noradrenergic cells in locus coeruleus (10), and dopaminergic cells in ventral tegmental area (11) can drive sleep-to-wake transitions. Hcrt cells send brain-wide projections that, in response to environmental cues, excite arousal nuclei by acting on one or both Hcrt receptors. Distinct wake-enhancing modulators promote distinct aspects of behavioral and cognitive arousal (11–13), but whether different wake-active cells or neuromodulator/receptor pairs differentially regulate waking electrocortical signatures or differently impact the sleep homeostat is poorly understood. In flies, striking differences are seen between wake induced by acetylcholine, dopamine, or octopamine cell activation on subsequent sleep (14). Among mammalian wake-enhancing neuromodulators, only Hcrt loss leads to a defined clinical condition, narcolepsy with cataplexy, characterized by sleep attacks, unstable nocturnal sleep, PS emergence into wake, and cataplexy. *Hcrt* knockout (*KO*) mice display all these symptoms, including an increase in state transitions, and thus model the behavioral state instability at the core of narcolepsy pathology (15). Untimed sleep, due to excessive daytime sleepiness, led early investigators to question the functional integrity of the sleep homeostat in narcolepsy. When patients were challenged by 24-h sleep deprivation (SD), subsequent time asleep and SWS δ power were, however, normal (16). Normal SWS δ power after 6-h SD was confirmed in the *Hcrt*$^{ko/ko}$ mouse model (15).

Significance

As in narcolepsy patients, overall time spent awake and asleep is normal in mice lacking the wake-enhancing neuromodulator hypocretin/orexin. We discovered, however, that these mice, in baseline conditions, are impaired in maintaining theta-dominated wakefulness (TDW), a waking substate characteristic of goal-driven, explorative behaviors and associated with heightened θ/fast-γ activity. We demonstrate that TDW instability causes profound blunting of EEG δ activity in subsequent slow-wave sleep, a measure gauging homeostatic sleep need. In contrast, manually enforced waking induced unimpaired TDW expression and normal δ activity in recovery sleep. This suggests that TDW, not overall waking, drives sleep need, a hypothesis we verified by modeling the homeostatic process. We propose that Hcrt is critical for spontaneous waking but that enforced waking relies on other neuromodulators, such as norepinephrine.

Author contributions: A.V. and P.F. designed research; A.V. and P.F. performed research; A.V. and P.F. analyzed data; and A.V. wrote the paper.

The authors declare no conflict of interest.

This article is a PNAS Direct Submission.

Freely available online through the PNAS open access option.

[1]To whom correspondence should be addressed. Email: anne.vassalli@unil.ch.

This article contains supporting information online at www.pnas.org/lookup/suppl/doi:10.1073/pnas.1700983114/-/DCSupplemental.

We confirm this finding but discover that, in SWS following their spontaneously most active waking period, $Hcrt^{ko/ko}$ mice display a severely reduced δ power, both relative to *WT* controls and to process-*S* simulation derived from prior sleep/wake history. This SWS δ power deficit is found to parallel reduced θ and fast-γ oscillatory dynamics in preceding wake. This led us to define a waking substate characterized by θ spectral dominance, theta-dominated wakefulness (TDW), which *KO* mice are unable to stably sustain in baseline and is associated with neural plasticity-related gene expression. In contrast, *KO* mice express normal TDW and θ/fast-γ activity when externally stimulated during SD. Using time in TDW to substitute time in all waking in process-*S* modeling, we predict SWS intensity solely based on TDW content of preceding wake. Thus, narcolepsy symptoms of daytime sleepiness and nighttime sleep fragmentation might be modeled in $Hcrt^{ko/ko}$ mice by a spontaneously unstable TDW state in active phase and diminished magnitude of δ oscillations in ensuing SWS.

Results

$Hcrt^{ko/ko}$ Mouse SWS Following Spontaneous Waking Shows Profound Blunting of EEG δ Power. Consistent with prior reports (15), $Hcrt^{ko/ko}$ mice responded to a 6-h SD with a prominent SWS δ power surge of similar dynamics and magnitude as *WT* mice. Surprisingly, however, in preceding baseline dark phases and night following SD, SWS δ activity of *KO* mice was severely diminished compared with *WT* controls (Fig. 1*A*, *Top*), although they both spent similar time in SWS (Fig. 1*A*, *Bottom*). $Hcrt^{ko/ko}$ mouse SWS δ activity only modestly increases in the first 3 dark h, although this time interval witnesses maximal wakefulness (see Fig. 3*A*) and locomotion (Fig. S1*B*) in *KO* as in *WT* mice.

What could explain *KO* mouse profound deficit in SWS δ activity after being awake in some contexts but not others? To assess whether this reflects *KO* mouse slightly lower total waking time in the first half of the night compared with *WT* mice (see Fig. 3*A*), thus predicting lower sleep need, we applied a mathematical simulation of the sleep homeostatic process *S* (2, 5). These initial simulations were run using parameters previously determined in mice of the same genetic background (17) (*Methods*). Simulations reproduced remarkably well the actual δ power values in *WT* mice (Fig. 1*A*, *Top*). In *KO* mice, however, actual values fell well below the simulation in dark phases. Hcrt loss thus severely disrupts the relationship between time spent spontaneously awake and subsequent SWS δ power.

We next reasoned that the shorter duration of SWS bouts in *KO* mice (Fig. S2*B*) may preclude a high-power δ rhythm to set in. We thus analyzed δ power kinetics surrounding SWS onset. In both genotypes, high-amplitude δ power was seen to rapidly set in, reaching a plateau in less than 30 s (Fig. 1*B*), thus ruling out SWS fragmentation as a cause for *KO* mouse δ power deficit. Because *KO* mouse baseline wake fails to raise sleep drive normally, we next set to determine whether alteration of its quality causes its different homeostatic weight.

Blunting of θ and Fast-γ Oscillations in Dark-Phase Spontaneous Wake of $Hcrt^{ko/ko}$ Mice. Dynamic analysis of the full waking EEG spectrum in the 3-d recording reveals that most salient changes occur in θ (6.0 to 9.5 Hz), slow-γ (32 to 45 Hz), and fast-γ (55 to 80 Hz) (18) (Fig. 2*B*). Behaviorally most active periods, namely early night and SD, display a sharp concerted increase in θ and fast-γ power and a modest slow-γ increase in both genotypes (Fig. 2*C*). $Hcrt^{ko/ko}$ mice, however, display greatly diminished θ (Fig. 2*C*, *Top*) and fast-γ (Fig. 2*C*, *Bottom*) power in baseline dark relative to *WT*, whereas slow-γ is unchanged (Fig. 2*C*, *Middle*). During SD, in contrast, which features the highest θ/fast-γ power of the 3 d, *KO* mice display θ/fast-γ power surges of similar magnitude as *WT* mice (Fig. 2*C*).

We next compared waking spectra in baseline early dark [Zeitgeber (ZT)12 to 18], when *KO* mice show severe SWS δ deficit, and 6-h SD, followed by normal SWS δ power. In baseline dark, *WT* mouse waking shows an ∼8-Hz θ peak that is absent in *KO*, in which an ∼5-Hz peak prevails (Fig. 2*A*, *Top*). During SD, in contrast, spectra feature a prominent ∼8-Hz θ rhythm in both genotypes (Fig. 2*A*, *Bottom*).

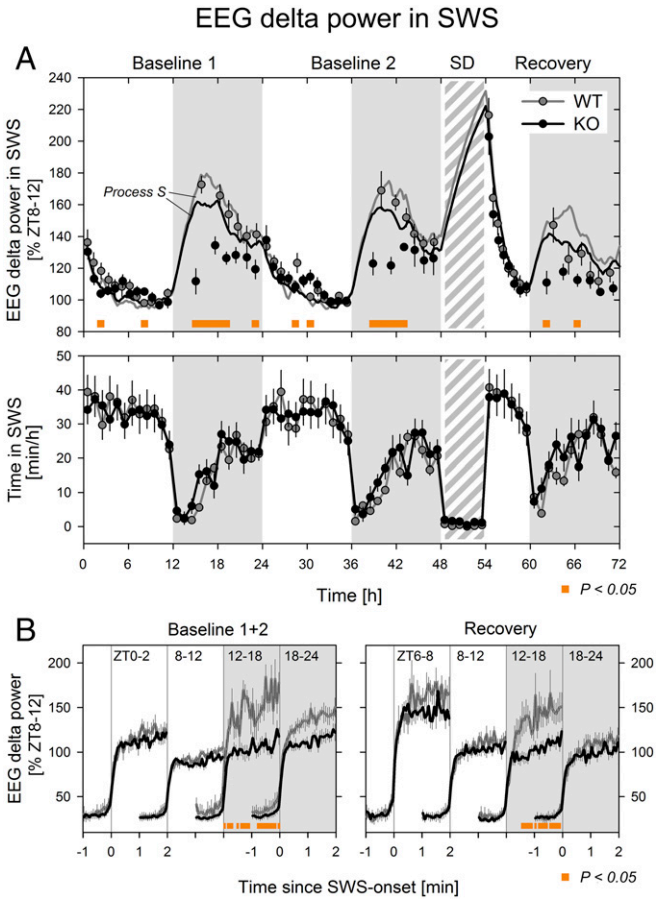

Fig. 1. $Hcrt^{ko/ko}$ mice display a profound deficit in EEG δ (1.0 to 4.0 Hz) power in baseline dark-phase SWS but respond to SD with an SWS δ power rebound indistinguishable from *WT* littermates. (*A*, *Top*) Dynamics of SWS δ power in $Hcrt^{ko/ko}$ and $Hcrt^{+/+}$ mice in the course of a 3-d recording with 6-h SD initiated at light onset of day 3 (ZT0 to 6). Mean δ power values (±SEM; *KO*, black symbols, $n = 8$; *WT*, gray symbols, $n = 7$) are expressed as the percentage of each mouse's mean SWS δ power in baseline ZT8 to 12. Solid curves (*KO*, black; *WT*, gray) represent process-*S* simulations calculated using published equation parameters (17). (*A*, *Bottom*) SWS (min/h) time course across the 3 d. (*B*) EEG δ power dynamics at state transitions to SWS, in the minute preceding and the 2 min following, SWS onset (time 0) in four baseline intervals (*Left*) and four recovery intervals (*Right*). Similar δ power levels are quickly reached in both genotypes at all times, except in early dark (ZT12 to 18), when *KO* mice show a reduced δ power plateau. Orange bars, intervals with significant genotype differences in δ power (*t* test, $P < 0.05$). In *B*, statistics concern only time after "time 0."

A Theta-Dominated Waking Substate. Rodent waking is often divided into quiet and active wake based on whether the animal is still or exhibits exploratory movements (1, 19). Transitions from quiet to active wake correlate with increased θ and γ power. Moreover, correlations between locomotion, waking θ, and subsequent SWS δ power are reported (4, 6), three variables found reduced in spontaneous waking of *KO* mice (for locomotion, see Fig. S1), suggesting that Hcrt has a role in active waking.

The blunting of θ/fast-γ power seen in baseline *KO* mouse waking might be due to spending less time in θ/fast-γ–rich wake or to a global weakened ability to generate θ/fast-γ oscillations.

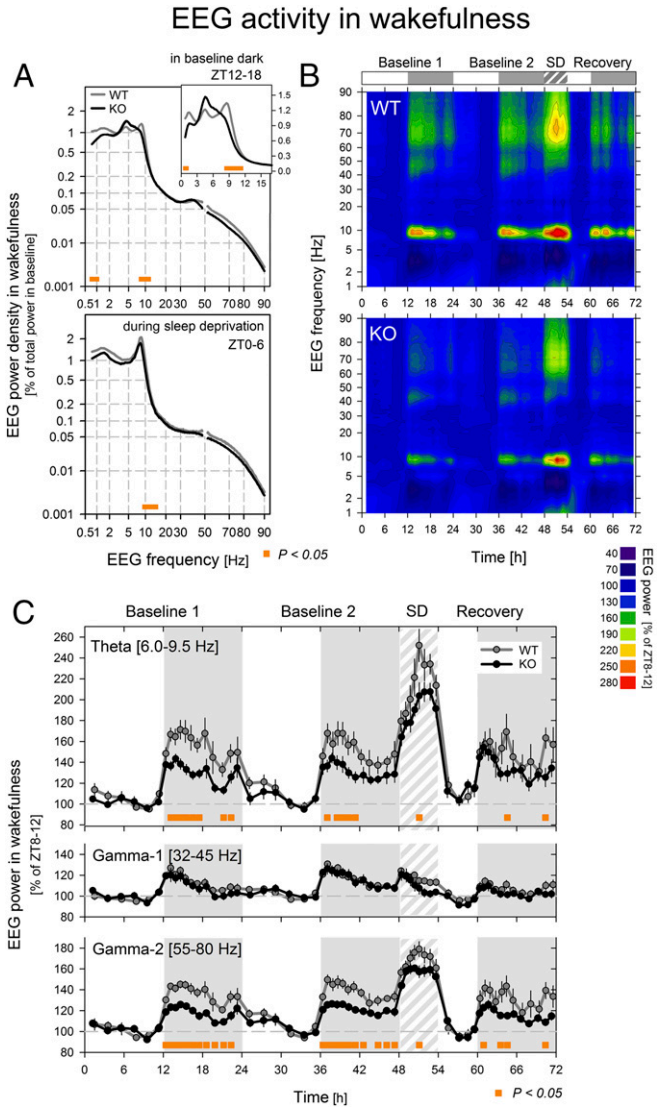

Fig. 2. Waking EEG θ (6.0 to 9.5 Hz) and fast-γ (55 to 80 Hz) oscillatory activities of $Hcrt^{ko/ko}$ mice are markedly reduced in baseline dark phase but similar to *WT* mouse values in most of the 6-h SD. (*A*) EEG spectra of $Hcrt^{ko/ko}$ (n = 8) and $Hcrt^{+/+}$ littermates (n = 7) in (*Top*) dark-phase spontaneous waking (ZT12 to 18) and (*Bottom*) enforced waking (ZT0 to 6). EEG power density values are expressed as the percentage of each mouse's total baseline EEG power (*SI Methods*). Note the nonlinear axes. (*A*, *Top*, *Inset*) Blowup of EEG spectra in the 0- to 16-Hz range. Axes here are linear. Orange bars, frequency bins with significant genotype differences in power density (t test, $P < 0.05$). (*B*) Heatmap of the spectral dynamics of the waking EEG across the 3 recorded days. Color-coded are mean waking EEG power density values across frequency bins, relative to each mouse's mean power density for that bin in waking of the baseline light-phase last 4 h (ZT8 to 12). Contour lines connect (frequency;time) pairs of equal relative EEG power density at 30% increments. Activity around 50 Hz (47.5 to 52.5 Hz) was eliminated and linearly interpolated. Changes are most pronounced in θ, slow-γ, and fast-γ power. Changes at ∼10 Hz result from an abrupt increase in TDW θ peak frequency at dark onset (Fig. S5). (*C*) Waking θ, slow-γ (Gamma-1), and fast-γ (Gamma-2) EEG power time course. Power value (±SEM) in the respective frequency range is expressed as in *B*. Orange bars, periods with significant genotype differences (t tests, $P < 0.05$).

To examine this, we designed an EEG-based algorithm that quantifies active waking, identified by the regular stereotypical θ rhythmic pattern, as seen in rodents engaged in goal-driven exploration (Fig. S3 and *Methods*). Video recordings were used to fine-tune defining parameters. The state thus identified was called theta-dominated wakefulness following a previously coined term (20).

Baseline TDW spectra of $Hcrt^{ko/ko}$ and $Hcrt^{+/+}$ mice were remarkably similar (Fig. 3*C*, *Left*). Furthermore, when TDW's θ and γ components were dynamically examined across the 3 d (as done above for all waking in Fig. 2*C*), we found the severe genotype differences to mostly vanish (Fig. S4). Namely, (*i*) the steep fluctuations in waking θ and fast-γ power across time and conditions were much reduced within the TDW state, and (*ii*) the pronounced genotype difference disappeared in θ and markedly diminished in fast-γ (Fig. S4). This strongly supports the efficacy of the TDW algorithm to capture a homogeneous waking substate, which is stable both among the two genotypes and across time and behavioral conditions.

Even though *KO* mouse TDW is qualitatively by and large normal, detailed analysis reveals differences. Whereas TDW in the two genotypes displays similar θ power (*KO* 1.74 ± 0.12% vs. *WT* 1.86 ± 0.18%; $P = 0.57$, t test), θ peak frequency is slower by half a Hz in *KO* mice (Fig. 3*D*, *Left*; *KO* 7.72 ± 0.10 vs. *WT* 8.21 ± 0.11; $P = 0.006$, t test). This *KO* mouse θ peak shift causes the ∼10-Hz power density deficit seen in Fig. 3*C* (*Left*) and also in the SD waking EEG (Fig. 2*A*, *Bottom*).

Applying the TDW algorithm across the 3 d revealed that, in their spontaneously most active phase (baseline dark), $Hcrt^{ko/ko}$ mice spend markedly less time (min/h) and fraction of total wake (%) in TDW, compared with *WT* controls (Fig. 3*A*). *WT* mice spent in total 3.55 ± 0.41 h per 12-h baseline night phase in TDW (30%), whereas *KO* mice spent only 2.05 ± 0.13 h in TDW (17%) ($P = 0.003$, t test). In contrast, during the 6-h SD, time in TDW did not differ (3.18 ± 0.33 and 2.98 ± 0.32 h, in *WT* and *KO*, respectively; $P = 0.67$, t test; Fig. 3*A*). *KO* mouse diminished baseline TDW was due to both a reduced rate of W-to-TDW transitions (−20%) and impaired TDW bout duration (−20%; Fig. 3*B*). A great number of TDW episodes lasted only for one epoch (4 s) (52 and 44%, in *KO* and *WT* mice, respectively; Fig. 3*B*) and, although the number of 4-s TDW bouts was similar in the two genotypes (*KO* 617; *WT* 651; Table S1 and Fig. 3*B*, *Top*), TDW bouts lasting longer than 4 s were over 40% fewer in *KO* mice than in controls ($P = 0.0006$, t test). $Hcrt^{ko/ko}$ mice thus appear impaired in effecting stable wake-to-TDW transitions and maintaining TDW network activity beyond 4 s.

In sum, Hcrt loss largely preserves the integrity of the TDW state EEG signature but compromises its stability, resulting in overall TDW state paucity. Because (*i*) TDW spectra are by and large normal, (*ii*) time spent in spontaneous TDW is reduced in *KO* mice, and (*iii*) genotype differences in θ/fast-γ dynamics disappear when analyzed within the TDW EEG, we conclude that the pronounced genotype differences in waking θ/fast-γ dynamics are not due to a reduced capacity to generate these rhythms but to engaging in a substate that supports their expression.

A Behavioral Validation of TDW. As mentioned above, $Hcrt^{ko/ko}$ mice reproduce the pathognomonic narcolepsy symptom of cataplexy. Cataplexy-triggering behaviors in mice are those typically associated with TDW, namely shelter construction and exploration. A behavioral analysis of the recordings presented here used EEG-independent, video-assessed criteria to identify cataplexy (21). Epochs that precede cataplexy typically match our video-independent, EEG-based TDW scoring criteria, thus offering a behavioral validation of the TDW definition. To further validate this relationship, we compared $Hcrt^{ko/ko}$ mouse EEG spectra in (*i*) baseline dark TDW, (*ii*) the minute preceding cataplexy, and (*iii*) 6-h SD waking (Fig. 3*E*). The three spectra almost match each other, all featuring a major ∼8-Hz power peak. A notable difference is that baseline dark TDW and pre-cataplexy both share an additional peak at ∼40 Hz (slow-γ) that is absent in enforced wake. $Hcrt^{+/+}$ mice are found to also express a slow-γ peak at similar frequency in baseline dark TDW (Fig. 3 *C* and *D*), although of a significantly lower power than *KO* (Fig. 3*F*).

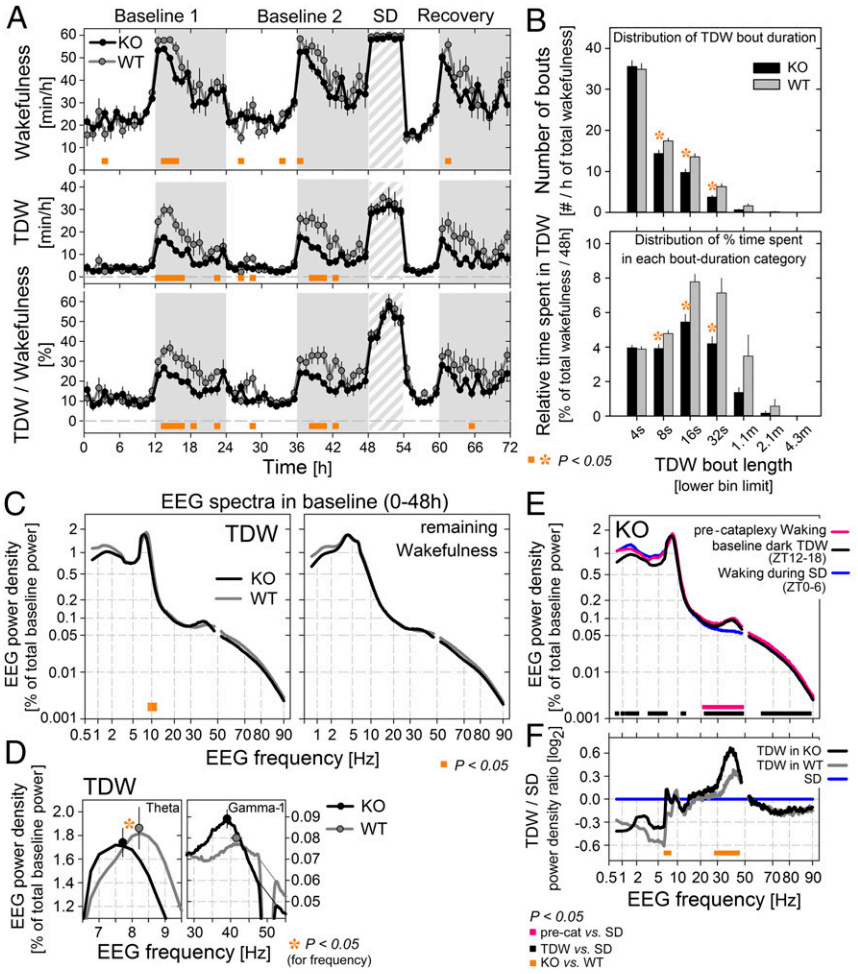

Fig. 3. TDW expression is impaired in $Hcrt^{ko/ko}$ mice. *KO* mice spend markedly less time in TDW in baseline dark phase than *WT* mice (*A*), due mainly to reduced TDW bout duration (*B*). They are, however, able to generate a TDW state spectrally similar to *WT* controls (*C*, *Left*), albeit of lower θ peak frequency (*D*) but higher slow-γ power (*F*). (*A*) Time courses of wake (min/h), TDW (min/h), and TDW as the percentage of total wake in $Hcrt^{ko/ko}$ (black; $n = 8$) and $Hcrt^{+/+}$ (gray; $n = 7$) mice. (*B*) Distribution of TDW bout duration (*Top*), and time spent in different bout-duration categories (*Bottom*). (*C*) EEG spectra in TDW (*Left*) and all other waking (*Right*) in baseline. Power density values are normalized as in Fig. 2*A*. Differences at ∼10 Hz stem from the slower TDW θ peak frequency in *KO* mice relative to *WT*. (*D*) Blowup of TDW spectra of *C*, with focus on θ and slow-γ (Gamma-1) power. Asterisks indicate significant genotype difference in frequency showing maximal power density (*t* test, $P < 0.05$). (*E*) EEG spectra of three types of *KO* mouse waking: minute preceding cataplexy (pink), baseline dark TDW (ZT12 to 18; black), and enforced waking (6-h SD; blue). A slow-γ peak (∼40 Hz) is seen in precataplexy and baseline dark TDW but not in SD. Horizontal bars, frequency bins with significant power density differences between baseline TDW and SD (black), or precataplexy and SD (pink) (*t* test, $P < 0.05$). (*F*) To emphasize differences between baseline dark TDW and SD wake, the TDW/SD EEG power density ratio is plotted across EEG frequency. Orange bars and asterisks indicate measures showing significant genotype differences (*t* test, $P < 0.05$).

This may be relevant to narcolepsy symptomatology, as β and slow-γ synchrony is seen in dopamine-depleted mice performing specific tasks and can correlate with motor dysfunction (22). We thus demonstrate that baseline dark and precataplexy define two spontaneous waking paradigms that rely on Hcrt to (*i*) stably express TDW, (*ii*) maintain normal TDW θ oscillatory frequency, and (*iii*) limit a concomitant slow-γ component.

TDW Is the Principal Driver of the Sleep Homeostat. Because $Hcrt^{ko/ko}$ mouse wake induces normal SWS δ power when its TDW content is normal (SD) but not when its TDW content is abnormally low (baseline), we sought to formally determine whether time in TDW more accurately predicts SWS intensity than total waking. To this end, we simulated process-*S* kinetics assuming *S* increases only in TDW rather than in all waking.

In initial simulations (Fig. 1*A*), we used for both genotypes parameters defined previously (17) (Table 1, model 1). Here we further optimized the parameters in each mouse to best fit the actual δ power measures. Assuming *S* increases in wake and PS, *S* evolves as in Fig. 4*B* (*Top*, solid curves) with equation parameters as in Table 1 (model 2). These *S* values match actual values with an excellent fit at all time points in *WT* mice. In *KO* mice, however, the simulation fails, in particular in light phase, as it "attempts" to fit the low δ power values measured in dark phase by underestimating expectation in light phase. Moreover, values obtained for τi and τd significantly differ in *KO* and *WT* mice. To assume that *S* increases in all types of wake (and PS) thus leads to invoking an alteration of processes regulating sleep homeostasis in *KO* mice. In contrast, modeling assuming that *S* increases solely in TDW predicts *S* increase and decrease rates that are similar in both genotypes (Table 1, model 3) and a better fit in *KO* mice (Fig. 4*B*, *Bottom*), whereas the fit stays excellent in *WT* mice. Because *KO* mice respond to 6-h SD with an SWS δ power rebound similar to *WT* controls, and because no evidence exists for altered process-*S* kinetics in narcolepsy (15, 16), an alteration of τi and τd rates in *KO* mice, as would result from model 2, is not favored. Our data most fit the hypothesis that *S* increases specifically in TDW and that sleep homeostatic processes are unimpaired in *KO* mice (model 3). Sleep homeostatic drive is thus primarily caused by events occurring in TDW, which accounts for only 18% of baseline recording [*WT* 4.38 ± 0.52 h (18.2%); *KO* 2.78 ± 0.19 h (11.6%); $P = 0.0094$, *t* test].

***Hcrt*$^{ko/ko}$ Mouse δ Deficit in SWS Affects Predominantly the Slow-δ Frequency Range.** We found that the SWS δ power deficit of *KO* mice in baseline dark is not equally distributed across the δ (1.0 to 4.0 Hz) range but mostly impacts slow-δ (δ1; 1.0 to 2.25 Hz) whereas fast-δ (δ2; 2.5 to 4.0 Hz) is less impaired, resulting in a greatly increased fast/slow (δ2/δ1) power ratio relative to *WT* (Fig. 5 *A* and *B*, *Left*). In contrast, the first 20 min of SWS after SD display high power in both δ components in *KO* as in *WT* mice, thereby normalizing *KO* mouse δ2/δ1 ratio (Fig. 5 *A* and *B*, *Right*). Interestingly, an SWS slow-δ deficit is also seen in recovery sleep of norepinephrine-depleted rats, and found, as shown below in our mice, to correlate with reduced expression of neural plasticity genes in preceding wake (23).

TDW: Not Just a Proxy of Locomotor Activity! Because prominent θ typically accompanies locomotion, we analyzed the interdependency of the TDW state and locomotor activity (LMA). As

Table 1. Equation parameters used in process-*S* modeling

Parameters	*KO*	*WT*	*P*
Model 1: Process *S* increases when not in SWS (in W+PS)			
Parameters as in Franken et al. (17) (Fig. 1*A*, *Top*)			
τI, h	7.9	7.9	—
τd, h	1.9	1.9	—
LA, %	55	55	—
UA, %	282	282	—
Fit, Δ%	23.9 ± 1.9	17.3 ± 2.5	0.049*
Model 2: Process *S* increases when not in SWS (in W+PS)			
Parameters individually optimized (Fig. 4*B*, *Top*)			
τI, h	17.6 ± 1.0	10.3 ± 1.7	0.0025*
τd, h	2.4 ± 0.2	1.7 ± 0.2	0.0094*
LA, %	47 ± 8	61 ± 6	0.20
UA, %	418 ± 22	361 ± 36	0.19
Fit, Δ%	14.0 ± 2.0	9.2 ± 1.3	0.078
Model 3: Process *S* increases in TDW exclusively			
Parameters individually optimized (Fig. 4*B*, *Bottom*)			
τI, h	4.3 ± 0.4	3.5 ± 0.4	0.13
τd, h	1.8 ± 0.3	1.4 ± 0.1	0.34
LA, %	80 ± 6	89 ± 3	0.24
UA, %	331 ± 22	310 ± 26	0.55
Fit, Δ%	12.7 ± 1.8	10.1 ± 1.7	0.33

Parameters yielding the best fit with actual EEG δ power dynamics are listed (mean ± SEM; *KO*, $n = 8$; *WT*, $n = 7$). In model 1 (Fig. 1*A*, *Top*), *S* is estimated using published parameters (17). For models 2 (Fig. 4*B*, *Top*) and 3 (Fig. 4*B*, *Bottom*), parameters were individually optimized in each mouse. Whereas *S* increases in W and PS in models 1 and 2, *S* increases exclusively in TDW in model 3. The third column lists *P* values for differences in parameter values between the two genotypes (underscored; *t* test, $*P < 0.05$). To quantify fit (Δ%), the mean % difference between simulated and observed δ power values across all time points is listed. Only model 3 yields a close fit in both genotypes and with similar parameters.

previously reported (24), locomotion in baseline dark phase is reduced in $Hcrt^{ko/ko}$ mice (Fig. S1*B*). During SD, LMA rose to higher counts than in early dark phase in both genotypes, but *KO* mice remained less active than *WT* controls. Linear regression indicated that TDW and LMA are globally strongly correlated in both genotypes, although the slope of the relation is significantly less steep in *KO* mice (Fig. S1*C*), indicating that not only do these mice spend less time in TDW but they are also less active per unit of time in TDW. Examination of the TDW–LMA relationship across the 3 d, however, revealed discrepancies. Whereas LMA is reduced in *KO* mice both in spontaneous and enforced waking (Fig. S1*B*), TDW expression is impaired in baseline but fully normal during SD. Thus, TDW can uncouple from movement. A high-resolution comparison of TDW and LMA in a representative *WT* mouse further supports this conclusion (Fig. S1*A*). We next assessed TDW prevalence during waking with LMA, and LMA prevalence in the TDW state (see Fig. S1*D* for details). Results showed that TDW is a better predictor of LMA (Fig. S1*D*, *Bottom*) than LMA is a predictor of the TDW state (Fig. S1*D*, *Top*), as TDW monitoring could capture both the genotype and dark/light differences in LMA expression, whereas LMA monitoring could not. Altogether, we conclude that time in TDW, not LMA, correlates with SWS EEG δ power, and thus is potentially causally linked to sleep homeostatic drive.

***$Hcrt^{ko/ko}$* Mice Show Reduced Cortical Expression of Neuronal Activity-Related Genes in Early Dark Phase.** We next examined whether reduced TDW expression and sleep homeostatic drive correlate with altered cortical expression of neuronal activity-induced genes or genes whose expression increases with explorative behavior (4) or enforced waking (25). *Arc*, *Bdnf*, *Egr1* (also known as *NgfiA* or *Zif268*), *Fos*, *Homer1a*, *Hspa5* (also known as *Bip*), and *Per2* transcripts were assayed either 1 h before dark onset (ZT11), when mice are fully rested after the major sleep period and SWS δ power is lowest, or 3 h into the dark phase (ZT15), when SWS δ power shows maximal deficit in $Hcrt^{ko/ko}$ mice. To further understand the impact of external stimulation on waking variables, mice were either subjected to a 3-h "SD" from dark onset to ZT15 (group ZT15+SD) or left undisturbed (group ZT15−SD).

In late resting phase (ZT11), levels of all seven transcripts were low, and indistinguishable in *KO* and *WT* mice (Fig. 6). Up-regulation from ZT11 to ZT15 was observed for all transcripts in *WT* mice, as expected, as ZT 12 to 15 h witnesses maximal waking time in *WT* and *KO* mice (Fig. 3*A*). In *KO* mice, however, *Bdnf* transcript failed to increase, whereas the other six transcripts did show up-regulation, but levels reached at ZT15 were moderately, albeit as a group highly significantly, lower than *WT* mouse levels. In single-transcript comparisons, *Bdnf*, *Egr1*, and *Per2* mRNAs showed significantly lower ZT15 relative abundance in *KO* than *WT* mice (Fig. 6).

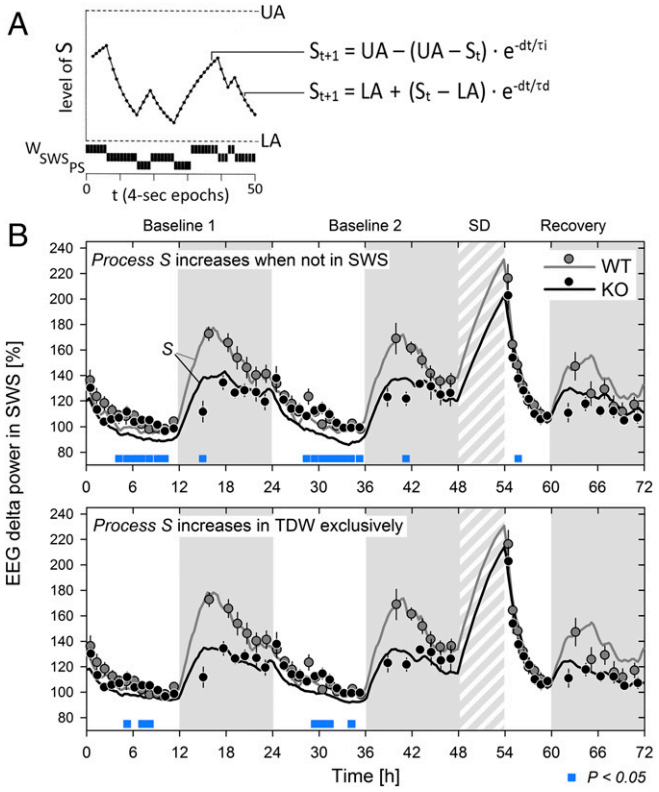

Fig. 4. Process-*S* modeling. (*A*) *S* is calculated iteratively in each 4-s epoch, based on the mouse's behavioral state sequence and two equations that feature four parameters. The *S* buildup equation is applied in W and PS (*B*, *Top;* model 2; Table 1) or exclusively in TDW (*B*, *Bottom*; model 3), and features an *S* increase rate (τi) time constant and an upper asymptote (UA; dashed line). The *S* decay equation is applied only in SWS in both models, and features an *S* decrease rate (τd) time constant and a lower asymptote (LA; dashed line). In each mouse, the four-parameter set yielding *S* values best fitting actual EEG data is determined (see Table 1 for parameters yielding the best fit). (*B*) Time course of process-*S* simulation and actual EEG δ power across the 3 d. Round symbols (black, *KO*, $n = 8$; gray, *WT*, $n = 7$) depict mean (±SEM) relative EEG δ power values. Curves depict mean process-*S* values. The "classical" model (*Top*) fails for $Hcrt^{ko/ko}$ mice in baseline light phase, and parameter best fitting asks for *S* buildup and decay rates to be slower in *KO* than in *WT* mice (Table 1). Fit markedly improves, and the *S* buildup and decay rate best-fitting parameters no longer differ between genotypes, when *S* is assumed to increase solely in TDW (*Bottom*). Blue bars, significant differences between measured and simulated values in $Hcrt^{ko/ko}$ mice (*t* test, $P < 0.05$). No differences are seen in $Hcrt^{+/+}$ mice.

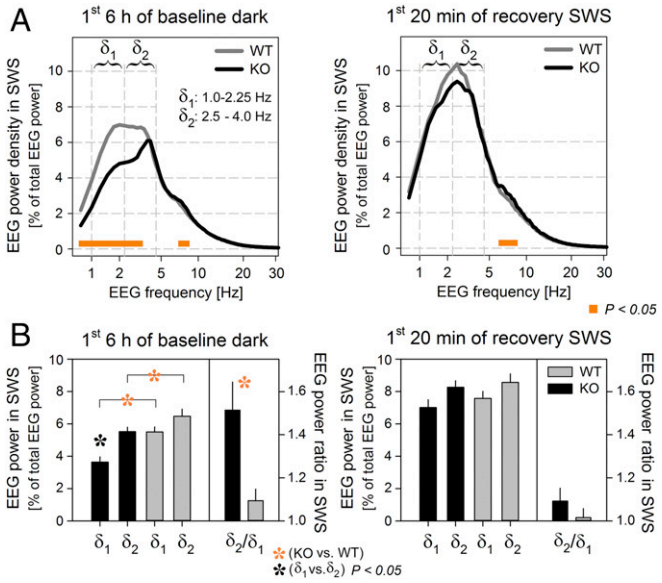

Fig. 5. SWS δ power deficit of *Hcrt*$^{ko/ko}$ mice in baseline dark phase affects predominantly slow-δ oscillations. (*A*) SWS EEG spectra in the first 6 h of baseline dark phase (ZT12 to 18; *Left*) and in the first 20 min of recovery after SD (*Right*) in *Hcrt*$^{+/+}$ (*WT*; gray, $n = 7$) and *Hcrt*$^{ko/ko}$ (*KO*; black, $n = 8$) mice. In baseline dark SWS, genotype differences are more pronounced in slow (δ1; 1.0 to 2.25 Hz) than in fast-δ (δ2; 2.5 to 4.0 Hz) power, whereas in recovery, *WT* and *KO* spectra largely overlap. Spectra are normalized as in Fig. 2*A*. Note the nonlinear frequency axis. (*B*, *Left*) In baseline SWS, *KO* mice show reduced power in both δ bands relative to *WT* but, unlike *WT* mice, power in slow-δ is significantly lower than in fast-δ (left ordinate; two-way rANOVA; genotype, $P = 0.0046$; δ band, $P = 0.0002$; interaction, $P = 0.049$), resulting in a vastly larger fast-to-slow δ power ratio (δ2/δ1 ratio; right ordinate) in *KO* mice. (*B*, *Right*) In recovery SWS, both fast- and slow-δ power, as well as fast-to-slow ratio, are restored to *WT* levels (two-way rANOVA; genotype, $P = 0.51$; δ band, $P = 0.024$; interaction, $P = 0.56$). Orange asterisks, power differences between genotypes (*t* test, $P < 0.05$); black asterisk, fast- vs. slow-δ power difference within genotype (paired *t* test, $P < 0.05$).

The 3-h SD condition up-regulated all transcripts in *KO* mice (group ZT15+SD vs. ZT15−SD), except *Egr1*, which in both *WT* and *KO* mice remained at ZT15 level irrespective of SD. It is noteworthy that external stimulation has the effect of normalizing the deficit of *KO* mice in baseline dark, not only at the EEG level (TDW expression, SWS δ power, δ2/δ1 ratio) but also at the molecular level, as all seven transcripts reached *WT* levels in *KO* mice after 3-h SD.

We then simulated process *S* for these experimental conditions, assuming *S* builds up in TDW only (Fig. 4*B*, *Bottom* and Table1, model 3). Results revealed how the dynamics of the seven transcripts tend to parallel those of the simulated sleep homeostatic drive (Fig. 6), with *Bdnf* most closely matching process *S*, consistent with prior reports (4).

Discussion

Here we provide an EEG-based algorithm that allows quantifying an active waking state, TDW, that we show by modeling to drive wake-dependent increase in sleep need and SWS δ power. We moreover show that, in spontaneously motivated arousal, TDW stability critically relies on Hcrt, possibly through Hcrt-dependent neuromodulation of circuits generating θ and fast-γ oscillations. Hence, Hcrt loss in *Hcrt*$^{ko/ko}$ mice results in TDW state instability and reduced SWS intensity that may model, respectively, the excessive daytime sleepiness and poor sleep quality of narcolepsy.

Hcrt Is an Essential Regulator of the EEG Determinants of Spontaneous Waking. We uncovered previously unseen alterations in spontaneous waking of *Hcrt*$^{ko/ko}$ mice by discovering unexpected features

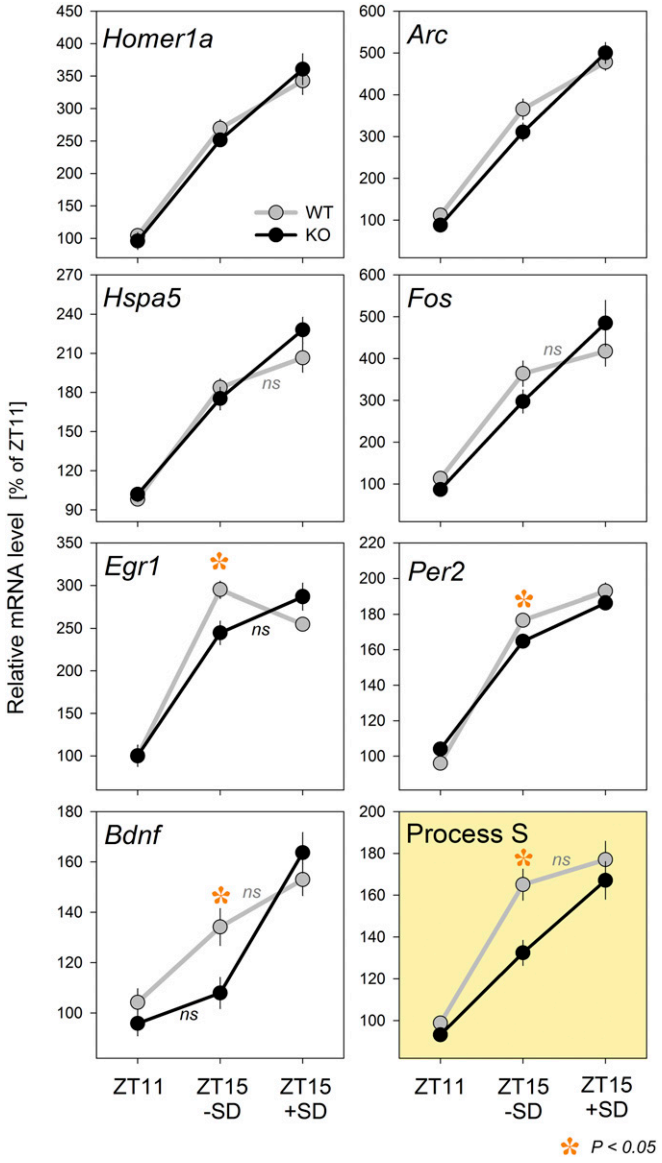

Fig. 6. Cortical expression of seven genes known to be up-regulated after prolonged waking. mRNA level was quantified in three groups of *Hcrt*$^{ko/ko}$ (black) and *Hcrt*$^{+/+}$ (gray) mice ($n = 7$ to 9 per group per genotype). Two groups were left undisturbed and killed either 1 h before (ZT11) or 3 h after dark onset (ZT15−SD). A third group (ZT15+SD) was sleep-deprived between ZT12 and 15 and then killed. Values (±SEM) are expressed as the percentage of mean mRNA level at ZT11. Gene expression increased significantly from ZT11 to 15 in both genotypes, except if labeled *ns* (nonsignificant). Transcript levels in ZT15−SD were lower in *KO* than in *WT* mice (two-way rANOVA; factor genotype, $P = 0.031$; factor transcript, $P < 0.0001$; interaction, $P = 0.29$), although post hoc test is significant for *Egr1*, *Per2*, and *Bdnf* only (orange asterisks; *t* test, $P < 0.05$). SD increased levels further (group ZT15+SD vs. ZT15−SD), and this effect was more pronounced in *KO* than in *WT* mice (two-way ANOVA; factor group, $P < 0.005$ for all transcripts, except *Egr1*, $P = 0.94$; factor genotype, $P > 0.29$ for all transcripts, except *Per2*, $P = 0.017$; interaction: *Egr1*, $P = 0.0022$; *Bdnf*, $P = 0.016$; *Arc*, *Fos*, and *Hspa5*, $P < 0.11$) (9). ZT15+SD mRNA levels did not differ between genotypes, indicating that SD normalizes *KO* mouse phenotype. (*Bottom Right*) Process *S* is modeled, assuming *S* increases only in TDW. For ZT15+SD data points, the simulation uses EEG data collected across ZT12 to 15 in *C57BL/6J WT* mice sleep-deprived across ZT12 to 18 (77), assuming that TDW expression during SD does not differ between genotypes, as for ZT0 to 6 SD (Fig. 3*A*).

in their sleep EEG. We found baseline SWS δ power to be severely blunted relative to *WT* littermates and predictions of sleep's classic homeostasis model, in which SWS δ power (often conceptualized as "sleep need") increases with time awake and decreases with time in SWS (2, 5). $Hcrt^{ko/ko}$ mice were known to normally respond to an SD challenge (15); however, they were not previously thoroughly tested in spontaneous conditions.

Discrepancy between actual and process-*S* modeling-derived δ power suggested that Hcrt loss alters either (*i*) sleep homeostasis or (*ii*) spontaneous waking quality. Because $Hcrt^{ko/ko}$ mice mount a fully normal SWS rebound after SD, the latter explanation was favored. Moreover, SWS δ power was shown to depend not only on prior time awake but also on EEG activity and behavioral content (4, 6, 26). Stress incurred by social defeat, for instance, enhances SWS δ power (3). Furthermore, studies on the genetic determinants of sleep homeostasis revealed that SWS δ power buildup rate is positively correlated with mean waking EEG θ power in mouse inbred lines (5). We thus examined the spectral content of the waking EEG in *KO* and control mice, revealing severe blunting of θ and fast-γ power in baseline dark phase in *KO* mice. Both rhythms, however, reach maximal power during SD with similar relative intensity in *KO* as *WT* mice, indicating that mechanisms generating θ and fast-γ oscillations are functional and recruited through alternate pathways in Hcrt absence. Spontaneous wake thus drastically differs from "gentle handling"-enforced wake in Hcrt dependence, presumed arousal circuits, and homeostatic impact. This is reminiscent of studies in *Drosophila* suggesting that distinct arousal neuromodulators impart distinct processing modes in target circuits, with distinct homeostatic costs (14). Likewise, Hcrt involvement in arousal appears to be driven by context-dependent determinants and drive system-wide processes, such as θ and fast-γ network rhythms.

Impaired TDW Stability and Cataplexy in $Hcrt^{ko/ko}$ Mice. The blunted EEG θ dynamics displayed by *KO* mice while spontaneously awake suggested that active waking, known to display a dominant θ rhythm, is specifically impaired in Hcrt absence. To verify this hypothesis, we designed the TDW scoring algorithm, which revealed that *KO* mice spend spontaneously markedly less time in TDW than *WT* mice, whereas time in TDW is normal during SD. Reduced baseline TDW is due to reduced TDW bout number and duration, indicating that Hcrt loss impairs the ability to maintain the TDW state for 4 s or longer.

$Hcrt^{ko/ko}$ mice display many features of human narcolepsy, including cataplexy. It should be noted that TDW fragmentation in these mice is not a consequence of cataplexy attacks interrupting TDW bouts. Just as these mice generate bouts of spectrally normal TDW in early dark phase, they demonstrate normal TDW-associated behaviors (vigorous running, burying, nest building), which are cataplexy triggers. Cataplexy thus interrupts a fraction of *KO* mouse TDW bouts, and we indeed showed precataplexy waking to be enriched in EEG θ and γ activity relative to global dark-phase waking (21). However, overt cataplexy remains rare (ca. 23 episodes per 12-h dark phase) (21), compared with TDW episodes (1,193 per 24 h). Although we cannot formally rule out that TDW fragmentation is linked to motor dysfunction below the sensitivity of our cataplexy definition, state instability is a hallmark phenotype of $Hcrt^{kō/ko}$ mice (15), and evidence favors TDW fragmentation to result from intrinsic TDW state lability in Hcrt absence.

Updating Sleep-Need Modeling. Existence within the same animal of two types of wake with distinct sleep homeostatic weights provides an opportunity to probe for attributes of wakefulness, including EEG variables, substate composition, and underlying neural determinants, that link wake to the sleep homeostat and thus determine sleep need and recovery function. To formally address whether *KO* mouse TDW deficit accounts for their SWS δ deficit, we turned to process-*S* equations (5), substituting wake for TDW, that is, applying the *S* buildup term only in TDW and *S* decay term only in SWS. This yielded (*i*) similar values in *KO* and *WT* mice for *S* buildup and decay rates and upper and lower *S* asymptotes, consistent with the notion of intact sleep homeostatic processes in *KO* mice, and (*ii*) faithful SWS δ power value prediction for both genotypes and both waking paradigms.

Although process-*S* modeling fits *WT* mouse data almost perfectly, *KO* mouse values remain less fitted, in particular in light phase. How can our modeling be further improved? First, we show that *KO* mouse TDW has a slower θ rhythm and γ-range differences relative to *WT* mice. TDW θ frequency is also not constant even within a genotype but tightly modulated across circadian and behavioral contexts (*SI Text* and Fig. S5). Such θ rhythm variations may affect process-*S* dynamics. Driving *S* by the number of θ oscillations per unit of time, rather than by the total time in TDW, may address these issues. Second, TDW's γ oscillatory component may allow refining the TDW definition or process-*S* equations. Third, $Hcrt^{ko/ko}$ mice, similar to narcolepsy patients, tend to transition into PS prematurely (Fig. S6) and express more PS than *WT* in dark phase (Fig. S2). High selective pressure for PS was shown to suppress SWS δ content (27), and a PS contribution to process-*S* dynamics was recently proposed (28). Therefore, the impact of PS, as well as quiet waking, in SWS δ modeling needs to be explored.

Altogether, our model proposes that sleep intensity, as reflected in δ oscillatory activity, which remains the best measure we have of the physiological need for sleep, depends on time spent in TDW, a state associated with the highest motivational drive (29) and neuronal activity-dependent plasticity (4). Although a waking θ/SWS δ correlation was reported by us and others (4–6), we here show SWS δ to be primarily determined by a discrete, fairly homogeneous, behavioral state. These insights may be relevant to explaining differences among various SD methods in eliciting EEG δ power rebound in recovery sleep. We speculate that failure to induce a pronounced δ rebound in some cases (30) may be due to the fact that, although these protocols successfully maintain animals awake, they do not induce robust θ activity and TDW state, as we show our gentle handling protocol to do.

Behavioral, Cellular, and Molecular Correlates of the TDW State. What underlies the relation between the TDW mode of waking and SWS δ activity? In rodents, θ activity generally refers to 5- to 10-Hz oscillations of uncertain functional unity. Dynamics of θ in waking are complex and influenced by the animal's behavior. In quiet wake and automatic behaviors, low-frequency (~5.5-Hz), broad-bandwidth θ reflects sleep propensity in rodents (31, 32) and humans (33). In voluntary behaviors, such as explorative locomotion, foraging, and alert immobility, a higher-frequency (7- to 10-Hz), narrow-bandwidth θ rhythm of hippocampal origin appears (29, 34). Thus, θ can both reflect homeostatic sleep drive (in quiet wake) and contribute to it (in active wake). Whether these activities are related is unknown, but it is the latter we define as a discrete behavioral state (TDW) predicting sleep intensity. Interestingly, the behaviors typically associated with TDW, such as spontaneous exploration (35) or active waking in head-restrained rodents (36, 37), witness the highest Hcrt cell-firing rate. Lack of Hcrt signaling in brain circuits of actively exploring *KO* mice likely contributes to TDW episodes' premature ending. *KO* mouse cataplexies likewise are triggered in motivated activities associated with high θ/γ EEG power (21), and their incidence parallels TDW state prevalence in early dark phase. This suggests that Hcrt release is needed as mice enter TDW, not only to sustain θ/fast-γ network activity but also to preserve the state's functional integrity, including robust coupling to muscle tone.

We found that, although movement counts and TDW prevalence are globally highly correlated in both genotypes, the two variables uncouple during SD, suggesting TDW can be expressed in the absence of overt locomotion. TDW/LMA uncoupling is consistent with rat studies showing that prominent hippocampal θ typically accompanies vigorous locomotion but can exist in the

resting animal preceding or following a running bout (34, 38) or under high motivational drive (29). Thus, TDW can occur in the absence of LMA, and LMA in the absence of TDW also likely occurs, as automatic locomotor activity such as wheel running was found to be associated with reduced cortical firing rates compared with exploration (39). Therefore, our data argue that TDW is not a simple readout of motor activity but a more sensitive marker of motivated waking.

Whether and through which mechanisms TDW is causally linked to SWS δ power hinge on issues of network homeostasis across behavioral states. If sleep is a response to waking cellular events that "use dependently" cause sleep need (7, 26, 40) to serve synaptic homeostatic and/or mnemonic sleep functions (41–43), TDW is expected to capture the homeostatic determinants of the "cost of waking." In support of this, hippocampal θ activity is associated with heightened synaptic plasticity and memory-related potentiation, and long-term potentiation (LTP) in the hippocampus is optimally induced by θ rhythms resembling those seen in exploring animals (44). TDW may thus lead to θ-dependent increases in connectivity, which once in SWS result in enhanced δ synchrony (45, 46). Upon prolonged TDW, however, potentiation processes are expected to saturate, just as process-*S* dynamics themselves saturate. SD indeed is found to impair LTP capacity (47, 48) that only sleep can restore. Our molecular data support a role of TDW in synaptic plasticity, as $Hcrt^{ko/ko}$ mouse lower TDW expression correlates with lower cortical expression of the plasticity-related transcripts *Egr1*/*Zif268*, *Per2*, and *Bdnf*. Consistent with prior studies (4, 49), *Bdnf* mRNA displays the highest correlation with EEG δ power across light-to-dark transitions and the two genotypes. Interestingly, *KO* mouse altered early dark-phase wakefulness also correlates with markedly up-regulated plasma corticosterone (Fig. S7).

TDW State Heterogeneity: Hcrt Loss Finely Alters the TDW Oscillatory Spectrum. We found $Hcrt^{ko/ko}$ mice to express a TDW state with normal θ power but slower frequency than *WT* mice. Although TDW has by definition an almost monochromatic (~8-Hz) θ power spectrum, its in vivo expression is associated with other oscillatory activities, notably in the high-frequency range, that also get modified by Hcrt loss. In baseline dark TDW and the minute preceding cataplexy, waking EEG spectra are very similar, including in featuring a distinct slow-γ (40-Hz) peak that is more powerful in *KO* than *WT* mice. SD, which is highly enriched in TDW in both genotypes, however, lacks this slow-γ peak. This suggests that Hcrt-dependent, goal-driven behaviors, but not Hcrt-independent, SD-enforced ones, solicit slow-γ–associated events, which are exaggerated in mice lacking Hcrt, and perhaps in narcolepsy. Abnormally high β and slow-γ synchrony is associated with motor disorders, including Parkinson's disease (PD). Depletion of striatal dopamine also causes amplified β (11- to 15-Hz) and slow-γ (40- to 53-Hz) activity in mice (22). The "antimovement" β band of PD patients correlates with impaired movement, and decreases with therapy and functional improvement. The enhanced slow-γ power of *KO* mouse baseline TDW may likewise be linked to motor deficits such as partial cataplexy. Hcrt signaling appears thus critical to limiting slow-γ activity in baseline dark-phase TDW, whereas under SD other arousal pathways sustain a TDW state largely lacking this activity. Supporting this, locus coeruleus norepinephrine (NE) cell stimulation, as likely occurs in SD, suppresses β (12- to 20-Hz) and slow-γ (20- to 40-Hz) activity in rats (50).

TDW stability thus seems to be mediated by context-dependent arousal pathways. Self-motivated TDW critically relies on Hcrt, whereas enforced TDW is largely Hcrt-independent and may partly rely on NE and threat-avoidance pathways. That TDW during SD is Hcrt-independent is consistent with studies showing that after 2-h SD, Hcrt cells become inhibited by NE (51). As sleep pressure builds up, Hcrt cell activity may thus fade and arousal increasingly rely on other neuromodulators and circuits, such as NE pathways. Hcrt-dependent behaviors are also thought to share an outreaching, positive emotional component (12, 52), as seen in cataplexy's failed coupling of muscle tone to emotional arousal (53), whereas pain-avoidant behaviors appear less affected in Hcrt absence (52). Gentle handling during SD may also induce Hcrt-independent threat-avoiding pathways that preserve TDW stability, explaining TDW contextual dichotomy.

Hcrt Deficiency Affects the Spectral Quality of SWS. We show that spontaneous waking is followed by SWS with a specific deficit in slow-δ in $Hcrt^{ko/ko}$ mice. This is reminiscent of findings in rats depleted of cortical NE that likewise manifest a slow-δ deficit in SWS following 6-h SD (23). These rats, moreover, display reduced cortical expression of synaptic activity-associated genes in preceding wake (25) like our *KO* mice in baseline dark phase. What mechanism may underlie this selective slow-δ loss? Low NE or Hcrt neuromodulatory levels cause thalamocortical neurons to hyperpolarize, which Steriade and coworkers have shown to lead to faster δ oscillations (54), and hence a spectral right shift as seen in *KO* mouse SWS. Although these effects are robust, their impact on homeostatic recovery remains unclear.

Hcrt and θ/γ Network Activity. What are the Hcrt-dependent processes whose lack in $Hcrt^{ko/ko}$ mice leads to alter so profoundly the stability of the circuits generating θ and γ oscillations? Both anatomical and electrophysiological data support a link between Hcrt signaling and θ oscillations. Hcrt cells profusely innervate the medial septum and diagonal band of Broca in basal forebrain (BF), which are critical in pacing hippocampal θ, and also project to posterior cingulate and prefrontal cortices, which house cortical θ pacemakers (55). In BF, Hcrt excites both cholinergic and GABA septohippocampal neurons (56–59), two cell types important in θ regulation. The hippocampal θ rhythm during movement was recently shown to be orchestrated by networks of reciprocal connections between septal and hippocampal parvalbumin-positive (PV) GABA cells (60, 61). Hcrt is known to excite these septohippocampal PV cells and contribute to hippocampal θ enhancement and arousal. Investigating the role of Hcrt signaling in the regulation of these septohippocampal networks is warranted.

A direct role of Hcrt in cortical γ oscillations is supported by recent studies showing that Hcrt enhances glutamatergic input on, and firing rate of, mouse prefrontal cortex fast-spiking PV cells (62), a cell type whose firing is both necessary and sufficient for γ activity (63, 64). $Hcrt^{ko/ko}$ mouse poor ability to sustain TDW may thus partly reflect the impaired activity of these prefrontal cells during motivated behaviors, which in *WT* mice correlate with Hcrt release. Supporting this hypothesis, local infusion of an HCRTR1 antagonist selectively reduces γ power (65), whereas infusion of Hcrt leads to improved accuracy in high-attention demanding tasks (66), known to correlate with fast-γ power (67). Moreover, cortical fast-spiking PV cells are critically involved in network stability and prevention of seizure propagation (64, 68). Cortical networks may thus be more vulnerable to uncontrolled hypersynchronies in Hcrt absence, which may explain the frontal high-amplitude paroxysmal θ bursts we and others reported in Hcrt-deficient mice during cataplexy and PS (21, 69) and in narcoleptic children during cataplexy (21). Failure of Hcrt neurotransmission in cortical fast-spiking PV cells may contribute to destabilizing θ/fast-γ network activities that underlie the TDW state. Thus, an Hcrt-responding cell type well-positioned to stabilize the TDW state in both BF and cortex is the PV GABAergic neuron.

What Is Sleepiness? Heightened θ and fast-γ oscillations correlate with intensive exploration in rodents and mental concentration in humans (67), and are thought to provide temporal frames for neuronal excitability and spiking fluctuations, thus facilitating information transfer. TDW instability in $Hcrt^{ko/ko}$ mice may thus weaken sensorimotor coding. Cognitive performance has been difficult to assay in narcolepsy due to the confounding effect of sleepiness. Sleep, however, remains restorative and phasic arousal is preserved in patients (70), and sleepiness-independent

deficits were reported, including impaired perceptual encoding of stimuli, attention deficits in executive tasks, and impaired decision making (70–72). Neural substrates underlying sleepiness and subjective perception of sleep propensity while awake are largely unknown. Could TDW instability model aspects of sleepiness? Increased wake-to-SWS and SWS-to-wake transitions (15), and TDW fragmentation, may induce a feeling of sleepiness. It is worth noting in this context that the extent of the debilitating sleep attacks experienced by narcoleptic patients in a given day do not correlate with the preceding night sleep quality (73), emphasizing that, although commonly referred to as a sleep disorder, narcolepsy is primarily caused by weakened networks that sustain active waking, independent of sleep homeostatic processes and sleep amount.

Perspective. The $Hcrt^{ko/ko}$ mouse models two segregated types of waking, spontaneously motivated waking in early nocturnal phase and enforced waking, associated with diverging oscillatory activity profiles and sleep homeostatic weights. This stems from the two waking modes' differential Hcrt dependence, where only the former depends on Hcrt to sustain the θ/fast-γ network activity that defines active waking, or TDW. The TDW variable allows quantifying active wake in distinct behavioral contexts, and successfully predicts δ power dynamics in $Hcrt^{+/+}$ and $Hcrt^{ko/ko}$ mice, baseline and recovery SWS, by assuming that TDW drives the sleep homeostat. Sleep homeostatic drive is thus primarily caused by events representing only a third of waking time, and TDW bouts presumably frame in time the activity of the causal substrates for the elusive physiological need for sleep.

A recent study provided evidence supporting that synaptic homeostasis, specifically the firing rate rebound occurring in visual cortical neurons following monocular deprivation, occurs exclusively in active waking (19), in striking contrast to the "SHY" hypothesis, which holds synaptic homeostasis as sleep's major function (41). A test of this contention may be to expose $Hcrt^{ko/ko}$ mice to monocular deprivation and determine whether their reduced TDW expression correlates with a slower efficiency in restoring firing rates, relative to a *WT* control group. Moreover, TDW is distinguished from other states by its neuromodulatory signature, of which elevated Hcrt is a component, as Hcrt is maximally released in active waking (36) and by the θ/fast-γ oscillatory network activity we use to define it, and which in baseline nonredundantly depends on Hcrt. Hcrt signaling was shown to mediate synaptic plasticity in some contexts (74) and may also play a role in gating synaptic homeostatic events. Hence, testing Hcrt's potential role in synaptic homeostatic processes is a prerequisite for interpreting the above experiment.

Because TDW is also likely associated with learning and related potentiation events (46), the TDW state would confine in close temporal association Hebbian potentiation events, synaptic homeostatic events that the former may contribute to causing to ensure network sustainability, and events determining sleep need, and thus potentially causally linked to SWS recovery functions. Elucidations of the mechanisms through which Hcrt signaling, in concert with other neuromodulators, affects the function of wake-active cortical networks in the healthy brain and neurological disorders are major goals of future research.

Methods

Mice. All analyses are based on comparing littermate $Hcrt^{ko/ko}$ (*KO*) and $Hcrt^{+/+}$ (*WT*) 3-mo-old males that were offspring of heterozygous $Hcrt^{tm1Ywa}$ ($Hcrt^{+/ko}$) parents (75). Mice were bred at the 10th *C57BL/6J*-backcross generation. Recordings described here were analyzed for cataplexy in a separate study (21). Differential frontoparietal EEG/EMG (electromyogram) data were acquired and analyzed as described (76) (see *SI Methods* for details).

All animal procedures followed Swiss federal laws and were preapproved by the State of Vaud Veterinary Office. At all times care was taken to minimize animal discomfort and avoid pain.

Theta-Dominated Wakefulness. An algorithm was created that analyzes the EEG of each 4-s epoch scored as waking, and identifies those meeting TDW-defining criteria. If the frequency bin with the highest power density in the 3.5- to 15-Hz range is within the 6.5- to 12.0-Hz range, and the ratio of θ power in the TDW θ peak frequency ± 1-Hz range over total power across 3.5 to 45 Hz is above 0.228, then the epoch scores as TDW, if the three following criteria are met: (*i*) the epoch immediately preceding was scored as "W" or "TDW"; (*ii*) the epoch immediately following was not scored as SWS; and (*iii*) single-TDW epochs preceded and followed by three W epochs are excluded. The 0.228 θ-to-total power ratio was chosen because algorithmically determined TDW epochs using this threshold yielded the best match with epochs visually identified as active waking based on their stereotypical, regular EEG θ rhythmic signal, in two *WT* and one *KO* mice. Moreover, video-assessed intense behaviors that typically precede cataplexy (21), and exploration following cage change, correlated with TDW scoring. Effect of the choice of the 0.228 threshold on genotype differences in TDW expression is assessed in Fig. S3.

Process-*S* Simulation. *S* is iteratively calculated in each mouse based on its 4-s-by-4-s behavioral state scoring sequence, assuming that it increases as a saturating exponential in wake and PS epochs according to $S[t+1] = UA - (UA - S[t]) \times e^{-dt/\tau i}$ and decreases exponentially in SWS epochs according to $S[t+1] = LA + (S[t] - LA) \times e^{-dt/\tau d}$, where $S[t]$ and $S[t+1]$ are consecutive *S* values, which vary between upper (*UA*) and lower (*LA*) asymptotes, with rate constants τi and τd, for *S* increase and decrease, respectively (5). The *S* simulation shown in Fig. 1*A* (*Top*) was performed using published τi, τd, UA, and LA parameter values (17). Subsequent simulations optimized the parameters in each mouse by searching for values yielding the best fit with measured δ power values. Fit was quantified as the least of the mean square of the differences upon running the simulation ∼200,000 times per mouse across the 3 d with a wide range of values for the four free parameters (Fig. 4*B*, *Top*). *S* value at $t = 0$ ($S[0]$) was estimated assuming that the 2 baseline days represent the steady state. For each four-parameter set, the simulation was run first for the two baselines with $S[0]$ set at 148% (17). *S* average at the end of each of the two baselines was used as $S[0]$ to initiate the final 3-d simulation. Optimization was based on 2 × 18 time intervals in baseline and 14 time intervals in recovery as the SWS δ power time course. This was repeated assuming *S* increases only in TDW and decreases only in SWS (Fig. 4*B*, *Bottom*). To draw the resulting time courses, process-*S* values were averaged at 15-min intervals.

Quantitative RT-PCR. PCRs were performed using both custom-designed and commercial TaqMan primers on an ABI PRISM 7900 HT real-time thermocycler (see *SI Methods* for details).

Statistics. TMT Pascal Multi-Target5 software (Framework Computers Inc.) was used to process data, SigmaPlot version 10.0 (Systat Software Inc.) was used for graphics, and SAS version 9.2 (SAS Institute Software Inc.) was used for statistics. Genotype effect on sleep/wake distribution, EEG power, and time course was assessed using two- or three-way repeated-measures analysis of variance (rANOVA). Genotype and time-of-day effects on mRNA level and plasma corticosterone were evaluated by ANOVA. Significant effects and interactions were decomposed using post hoc Tukey's honest significance and *t* tests. Statistical significance was set at $P = 0.05$, and results are reported as mean ± SEM.

ACKNOWLEDGMENTS. We thank Masashi Yanagisawa and Takeshi Sakurai for the mice; Mehdi Tafti, Peter Achermann, and Cyril Mykhail for insightful discussions; and Christina Schrick and Yann Emmenegger for superb technical assistance. This work was supported by grants from the Swiss National Science Foundation (144282 to A.V.; 130825 and 146694 to P.F.) and by the State of Vaud, Switzerland (to P.F.).

1. McGinley MJ, et al. (2015) Waking state: Rapid variations modulate neural and behavioral responses. *Neuron* 87:1143–1161.
2. Daan S, Beersma DG, Borbély AA (1984) Timing of human sleep: Recovery process gated by a circadian pacemaker. *Am J Physiol* 246:R161–R183.
3. Meerlo P, Pragt BJ, Daan S (1997) Social stress induces high intensity sleep in rats. *Neurosci Lett* 225:41–44.
4. Huber R, Tononi G, Cirelli C (2007) Exploratory behavior, cortical BDNF expression, and sleep homeostasis. *Sleep* 30:129–139.
5. Franken P, Chollet D, Tafti M (2001) The homeostatic regulation of sleep need is under genetic control. *J Neurosci* 21:2610–2621.
6. Leemburg S, et al. (2010) Sleep homeostasis in the rat is preserved during chronic sleep restriction. *Proc Natl Acad Sci USA* 107:15939–15944.

7. Krueger JM, Tononi G (2011) Local use-dependent sleep; synthesis of the new paradigm. *Curr Top Med Chem* 11:2490–2492.
8. Jones BE (2003) Arousal systems. *Front Biosci* 8:s438–s451.
9. Adamantidis AR, Zhang F, Aravanis AM, Deisseroth K, de Lecea L (2007) Neural substrates of awakening probed with optogenetic control of hypocretin neurons. *Nature* 450:420–424.
10. Carter ME, et al. (2010) Tuning arousal with optogenetic modulation of locus coeruleus neurons. *Nat Neurosci* 13:1526–1533.
11. Eban-Rothschild A, Rothschild G, Giardino WJ, Jones JR, de Lecea L (2016) VTA dopaminergic neurons regulate ethologically relevant sleep-wake behaviors. *Nat Neurosci* 19:1356–1366.
12. Blouin AM, et al. (2013) Human hypocretin and melanin-concentrating hormone levels are linked to emotion and social interaction. *Nat Commun* 4:1547.
13. Anaclet C, et al. (2009) Orexin/hypocretin and histamine: Distinct roles in the control of wakefulness demonstrated using knock-out mouse models. *J Neurosci* 29: 14423–14438.
14. Seidner G, et al. (2015) Identification of neurons with a privileged role in sleep homeostasis in *Drosophila melanogaster*. *Curr Biol* 25:2928–2938.
15. Mochizuki T, et al. (2004) Behavioral state instability in orexin knock-out mice. *J Neurosci* 24:6291–6300.
16. Tafti M, Rondouin G, Besset A, Billiard M (1992) Sleep deprivation in narcoleptic subjects: Effect on sleep stages and EEG power density. *Electroencephalogr Clin Neurophysiol* 83:339–349.
17. Franken P, et al. (2006) NPAS2 as a transcriptional regulator of non-rapid eye movement sleep: Genotype and sex interactions. *Proc Natl Acad Sci USA* 103:7118–7123.
18. Hasan S, et al. (2009) How to keep the brain awake? The complex molecular pharmacogenetics of wake promotion. *Neuropsychopharmacology* 34:1625–1640.
19. Hengen KB, Torrado Pacheco A, McGregor JN, Van Hooser SD, Turrigiano GG (2016) Neuronal firing rate homeostasis is inhibited by sleep and promoted by wake. *Cell* 165:180–191.
20. Welsh DK, Richardson GS, Dement WC (1985) A circadian rhythm of hippocampal theta activity in the mouse. *Physiol Behav* 35:533–538.
21. Vassalli A, et al. (2013) Electroencephalogram paroxysmal θ characterizes cataplexy in mice and children. *Brain* 136:1592–1608.
22. Lemaire N, et al. (2012) Effects of dopamine depletion on LFP oscillations in striatum are task- and learning-dependent and selectively reversed by L-DOPA. *Proc Natl Acad Sci USA* 109:18126–18131.
23. Cirelli C, Huber R, Gopalakrishnan A, Southard TL, Tononi G (2005) Locus ceruleus control of slow-wave homeostasis. *J Neurosci* 25:4503–4511.
24. Kayaba Y, et al. (2003) Attenuated defense response and low basal blood pressure in orexin knockout mice. *Am J Physiol Regul Integr Comp Physiol* 285:R581–R593.
25. Cirelli C (2009) The genetic and molecular regulation of sleep: From fruit flies to humans. *Nat Rev Neurosci* 10:549–560.
26. Feinberg I, Thode HC, Jr, Chugani HT, March JD (1990) Gamma distribution model describes maturational curves for delta wave amplitude, cortical metabolic rate and synaptic density. *J Theor Biol* 142:149–161.
27. Beersma DG, Dijk DJ, Blok CG, Everhardus I (1990) REM sleep deprivation during 5 hours leads to an immediate REM sleep rebound and to suppression of non-REM sleep intensity. *Electroencephalogr Clin Neurophysiol* 76:114–122.
28. Hayashi Y, et al. (2015) Cells of a common developmental origin regulate REM/non-REM sleep and wakefulness in mice. *Science* 350:957–961.
29. Sławińska U, Kasicki S (1998) The frequency of rat's hippocampal theta rhythm is related to the speed of locomotion. *Brain Res* 796:327–331.
30. Rechtschaffen A, Bergmann BM, Gilliland MA, Bauer K (1999) Effects of method, duration, and sleep stage on rebounds from sleep deprivation in the rat. *Sleep* 22:11–31.
31. Franken P, Dijk DJ, Tobler I, Borbély AA (1991) Sleep deprivation in rats: Effects on EEG power spectra, vigilance states, and cortical temperature. *Am J Physiol* 261: R198–R208.
32. Vyazovskiy VV, Tobler I (2005) Theta activity in the waking EEG is a marker of sleep propensity in the rat. *Brain Res* 1050:64–71.
33. Finelli LA, Baumann H, Borbély AA, Achermann P (2000) Dual electroencephalogram markers of human sleep homeostasis: Correlation between theta activity in waking and slow-wave activity in sleep. *Neuroscience* 101:523–529.
34. McFarland WL, Teitelbaum H, Hedges EK (1975) Relationship between hippocampal theta activity and running speed in the rat. *J Comp Physiol Psychol* 88:324–328.
35. Mileykovskiy BY, Kiyashchenko LI, Siegel JM (2005) Behavioral correlates of activity in identified hypocretin/orexin neurons. *Neuron* 46:787–798.
36. Lee MG, Hassani OK, Jones BE (2005) Discharge of identified orexin/hypocretin neurons across the sleep-waking cycle. *J Neurosci* 25:6716–6720.
37. Takahashi K, Lin JS, Sakai K (2008) Neuronal activity of orexin and non-orexin waking-active neurons during wake-sleep states in the mouse. *Neuroscience* 153:860–870.
38. Vinck M, Batista-Brito R, Knoblich U, Cardin JA (2015) Arousal and locomotion make distinct contributions to cortical activity patterns and visual encoding. *Neuron* 86:740–754.
39. Fisher SP, et al. (2016) Stereotypic wheel running decreases cortical activity in mice. *Nat Commun* 7:13138.
40. Krueger JM, et al. (2008) Sleep as a fundamental property of neuronal assemblies. *Nat Rev Neurosci* 9:910–919.
41. Tononi G, Cirelli C (2006) Sleep function and synaptic homeostasis. *Sleep Med Rev* 10: 49–62.
42. Feld GB, Born J (2017) Sculpting memory during sleep: Concurrent consolidation and forgetting. *Curr Opin Neurobiol* 44:20–27.
43. Havekes R, Abel T (2017) The tired hippocampus: The molecular impact of sleep deprivation on hippocampal function. *Curr Opin Neurobiol* 44:13–19.
44. Wójtowicz T, Mozrzymas JW (2015) Diverse impact of neuronal activity at θ frequency on hippocampal long-term plasticity. *J Neurosci Res* 93:1330–1344.
45. Vassalli A, Dijk DJ (2009) Sleep function: Current questions and new approaches. *Eur J Neurosci* 29:1830–1841.
46. Vyazovskiy VV, Cirelli C, Tononi G (2011) Electrophysiological correlates of sleep homeostasis in freely behaving rats. *Prog Brain Res* 193:17–38.
47. Vyazovskiy VV, Cirelli C, Pfister-Genskow M, Faraguna U, Tononi G (2008) Molecular and electrophysiological evidence for net synaptic potentiation in wake and depression in sleep. *Nat Neurosci* 11:200–208.
48. Kuhn M, et al. (2016) Sleep recalibrates homeostatic and associative synaptic plasticity in the human cortex. *Nat Commun* 7:12455.
49. Hairston IS, et al. (2004) Sleep deprivation effects on growth factor expression in neonatal rats: A potential role for BDNF in the mediation of delta power. *J Neurophysiol* 91:1586–1595.
50. Brown RA, Walling SG, Milway JS, Harley CW (2005) Locus ceruleus activation suppresses feedforward interneurons and reduces beta-gamma electroencephalogram frequencies while it enhances theta frequencies in rat dentate gyrus. *J Neurosci* 25: 1985–1991.
51. Grivel J, et al. (2005) The wake-promoting hypocretin/orexin neurons change their response to noradrenaline after sleep deprivation. *J Neurosci* 25:4127–4130.
52. McGregor R, Wu MF, Barber G, Ramanathan L, Siegel JM (2011) Highly specific role of hypocretin (orexin) neurons: Differential activation as a function of diurnal phase, operant reinforcement versus operant avoidance and light level. *J Neurosci* 31: 15455–15467.
53. Burgess CR, Peever JH (2013) A noradrenergic mechanism functions to couple motor behavior with arousal state. *Curr Biol* 23:1719–1725.
54. Dossi RC, Nuñez A, Steriade M (1992) Electrophysiology of a slow (0.5-4 Hz) intrinsic oscillation of cat thalamocortical neurones in vivo. *J Physiol* 447:215–234.
55. Talk A, Kang E, Gabriel M (2004) Independent generation of theta rhythm in the hippocampus and posterior cingulate cortex. *Brain Res* 1015:15–24.
56. Gerashchenko D, Salin-Pascual R, Shiromani PJ (2001) Effects of hypocretin-saporin injections into the medial septum on sleep and hippocampal theta. *Brain Res* 913:106–115.
57. Wu M, et al. (2002) Hypocretin increases impulse flow in the septohippocampal GABAergic pathway: Implications for arousal via a mechanism of hippocampal disinhibition. *J Neurosci* 22:7754–7765.
58. Wu M, Zaborszky L, Hajszan T, van den Pol AN, Alreja M (2004) Hypocretin/orexin innervation and excitation of identified septohippocampal cholinergic neurons. *J Neurosci* 24:3527–3536.
59. Arrigoni E, Mochizuki T, Scammell TE (2010) Activation of the basal forebrain by the orexin/hypocretin neurones. *Acta Physiol (Oxf)* 198:223–235.
60. Hangya B, Borhegyi Z, Szilágyi N, Freund TF, Varga V (2009) GABAergic neurons of the medial septum lead the hippocampal network during theta activity. *J Neurosci* 29: 8094–8102.
61. Amilhon B, et al. (2015) Parvalbumin interneurons of hippocampus tune population activity at theta frequency. *Neuron* 86:1277–1289.
62. Aracri P, Banfi D, Pasini ME, Amadeo A, Becchetti A (2015) Hypocretin (orexin) regulates glutamate input to fast-spiking interneurons in layer V of the Fr2 region of the murine prefrontal cortex. *Cereb Cortex* 25:1330–1347.
63. Cardin JA, et al. (2009) Driving fast-spiking cells induces gamma rhythm and controls sensory responses. *Nature* 459:663–667.
64. Sohal VS, Zhang F, Yizhar O, Deisseroth K (2009) Parvalbumin neurons and gamma rhythms enhance cortical circuit performance. *Nature* 459:698–702.
65. He C, et al. (2015) Functional inactivation of hypocretin 1 receptors in the medial prefrontal cortex affects the pyramidal neuron activity and gamma oscillations: An in vivo multiple-channel single-unit recording study. *Neuroscience* 297:1–10.
66. Lambe EK, Olausson P, Horst NK, Taylor JR, Aghajanian GK (2005) Hypocretin and nicotine excite the same thalamocortical synapses in prefrontal cortex: Correlation with improved attention in rat. *J Neurosci* 25:5225–5229.
67. Buzsáki G (2006) *Rhythms of the Brain* (Oxford Univ Press, New York).
68. Cammarota M, Losi G, Chiavegato A, Zonta M, Carmignoto G (2013) Fast spiking interneuron control of seizure propagation in a cortical slice model of focal epilepsy. *J Physiol* 591:807–822.
69. Bastianini S, Silvani A, Berteotti C, Lo Martire V, Zoccoli G (2012) High-amplitude theta wave bursts during REM sleep and cataplexy in hypocretin-deficient narcoleptic mice. *J Sleep Res* 21:185–188.
70. Rieger M, Mayer G, Gauggel S (2003) Attention deficits in patients with narcolepsy. *Sleep* 26:36–43.
71. Henry GK, Satz P, Heilbronner RL (1993) Evidence of a perceptual-encoding deficit in narcolepsy? *Sleep* 16:123–127.
72. Bayard S, et al. (2011) Decision making in narcolepsy with cataplexy. *Sleep* 34:99–104.
73. Tafti M, Villemin E, Carlander B, Besset A, Billiard M (1992) Sleep onset rapid-eye-movement episodes in narcolepsy: REM sleep pressure or nonREM-REM sleep dysregulation? *J Sleep Res* 1:245–250.
74. Yang L, et al. (2013) Hypocretin/orexin neurons contribute to hippocampus-dependent social memory and synaptic plasticity in mice. *J Neurosci* 33:5275–5284.
75. Chemelli RM, et al. (1999) Narcolepsy in orexin knockout mice: Molecular genetics of sleep regulation. *Cell* 98:437–451.
76. Mang GM, Franken P (2012) Sleep and EEG phenotyping in mice. *Curr Protoc Mouse Biol* 2:55–74.
77. Curie T, et al. (2013) Homeostatic and circadian contribution to EEG and molecular state variables of sleep regulation. *Sleep* 36:311–323.
78. Rowe K, et al. (1999) Heart rate surges during REM sleep are associated with theta rhythm and PGO activity in cats. *Am J Physiol* 277:R843–R849.
79. Franken P, Malafosse A, Tafti M (1998) Genetic variation in EEG activity during sleep in inbred mice. *Am J Physiol* 275:R1127–R1137.
80. Franken P, Malafosse A, Tafti M (1999) Genetic determinants of sleep regulation in inbred mice. *Sleep* 22:155–169.